Geomorphometric Controls on Mountain Glacier Changes Since the Little Ice Age in the Eastern Tien Shan, Central Asia

Article · December 2016

DOI: 10.1080/24694452.2016.1248552

4 authors:


Yanan Li
Texas State University


Yingkui Li
University of Tennessee


Xiaoyu Lu
University of Tennessee


Jon Harbor
Purdue University

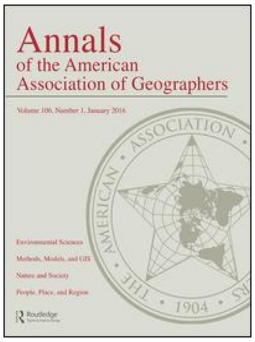

Annals of the American Association of Geographers

ISSN: 2469-4452 (Print) 2469-4460 (Online) Journal homepage: http://www.tandfonline.com/loi/raag21

Geomorphometric Controls on Mountain Glacier Changes Since the Little Ice Age in the Eastern Tien Shan, Central Asia

Yanan Li, Yingkui Li, Xiaoyu Lu & Jon Harbor

Geomorphometric Controls on Mountain Glacier Changes Since the Little Ice Age in the Eastern Tien Shan, Central Asia

Yanan Li,* Yingkui Li,† Xiaoyu Lu,† and Jon Harbor‡

**Department of Geography, South Dakota State University*
†Department of Geography, The University of Tennessee, Knoxville
‡Department of Earth, Atmospheric, and Planetary Sciences, Purdue University

The linkage between glacier change and climate has garnered significant attention in recent decades, but little is known about the role of local geomorphometric factors on glacier changes since the Little Ice Age (LIA), approximately 100 to 700 years ago. This study examines the spatial pattern of changes in glacier area in the eastern Tien Shan based on geomorphological mapping of LIA glacial extents and contemporary glaciers from the Second Glacier Inventory of China. Partial least squares regression was applied to examine the correlations between geomorphometric factors, including glacier area, slope, aspect, shape, elevation, and hypsometry, and relative glacier area loss, both in the whole area and in three subregions (the Boro-Eren Range, the Bogda Range, and the Karlik Range). Our results show that the area of 640 mapped LIA glaciers decreased from 791.6 ± 18.7 km^2 to 483.9 ± 31.2 km^2 between 2006 and 2010, a loss of 38.9 ± 2.7 percent. The losses for three subregions are 43.4 ± 3.2 percent, 35.9 ± 2.4 percent, and 30.2 ± 1.8 percent, respectively. Elevation, slope, and area of a glacier are the three most significant geomorphometric factors to glacier area change, at both regional and subregional scales. The west–east decreasing trend of glacier retreat and different variances explained in subregional regressions might reflect the influence from the shifting dominance of the westerlies and the Siberian High. *Key Words: eastern Tien Shan, geomorphometric factors, glacier change, Little Ice Age.*

冰川改变和气候之间的关联, 在近数十年来获得了显着的关注, 但我们对于大约一百至七百年前的小冰期(LIA)以降, 冰川改变的在地地形计测係数所扮演的角色却所知甚少。本研究根据中国第二次冰川编目中的小冰期冰河范围和目前冰川的地形计测製图, 检视天山东部冰川地区的空间模式变化。本文应用篇最小平方迴归, 检视在整个地区和在三大次区域中(博罗—依连山脉、博格达山脉、喀尔里克山脉), 包含冰川面积、坡度、坡向、形态、海拔和测高法的地形计测係数与冰川面积的相对丧失之间的相互关係。我们的研究结果显示, 六百四十个绘製的LIA冰川面积, 在 2006 年至 2010 年间, 从 791.6 ± 18.7 平方公里, 降至 483.9 ± 31.2 平方公里, 一共损失百分之38.9 ± 2.7。三大次区域的丧失各为百分之 43.4 ± 3.2, 百分之 35.9 ± 2.4, 以及百分之 30.2 ± 1.8。冰川的海拔、坡度和面积, 是区域及次区域尺度中冰川面积改变的三个最重要的地形计测係数。冰川后退的东西向减少趋势, 以及次区域迴归所解释的不同变异, 可能反映出西风带和西伯利亚高压支配转变的影响。 *关键词: 天山东部, 地形计测係数, 冰川改变, 小冰期。*

El nexo entre cambios de los glaciares y clima ha logrado atraer notable atención en décadas recientes, pero poco se sabe acerca del papel de factores geomorfométricos locales sobre los cambios glaciarios desde la Pequeña Edad del Hielo (PEH), aproximadamente entre 100 y 700 años atrás. Este estudio examina los cambios del patrón espacial en el área glaciada de la parte oriental del Tien Shan con base en cartografía geomorfológica de las extensiones glaciares de la PEH y de los glaciares contemporáneos del Segundo Inventario Glaciar de China. Se aplicó una regresión parcial de mínimos cuadrados para examinar las correlaciones entre factores geomorfométricos, incluyendo el área de los glaciares, la inclinación, aspecto, forma, elevación e hipsometría, y la pérdida relativa de área glaciaria, tanto en el área total como en tres subregiones (la Cordillera Boro-Eren, la Cordillera Bogda y la Cordillera Karlik). Nuestros resultados muestran que el área cartografiada de 640 glaciares de la PEH disminuyó de 791.6 ± 18.7 km2 a 483.9 ± 31.2 km2 entre 2006 y 2010, una pérdida de 38.9 ± 2.7 por ciento. Las pérdidas para las tres subregiones son 43.4 ± 3.2 por ciento, 35.9 ± 2.4 por ciento y 30.2% ± 1.8 por ciento, respectivamente. La elevación, la inclinación y el área de un glaciar son los tres factores geomorfométricos más significativos para el cambio de área del glaciar, tanto a escala regional como subregional. La tendencia oeste–este de recesión del glaciar y las diferentes varianzas explicadas en regresiones subregionales podrían reflejar la influencia del cambio de predominio de los vientos oestes y de la zona de Alta Presión de Siberia. *Palabras clave: Tien Shan oriental, factores geomorfométricos, cambio glaciario, Pequeña Edad del Hielo.*

Annals of the American Association of Geographers, 107(2) 2017, pp. 284–298 © 2017 by American Association of Geographers
Initial submission, February 2016; revised submission, June 2016; final acceptance, July 2016
Published by Taylor & Francis, LLC.

Glacier change is one of the manifestations of global climate change, especially in mountainous regions where meteorological data are scarce. Although glacier mass balances are mainly affected by the dominance of shifting climate controls, geomorphometric and glaciological factors also play significant roles in forming the spatial pattern of glacier changes (Furbish and Andrews 1984; DeBeer and Sharp 2007; K. Li et al. 2011; Delmas, Gunnell, and Calvet 2014). In particular, the difference in glacier size, aspect, shape, slope, elevation, and hypsometry could cause the heterogeneous response of glaciers to climate change in different regions. Assuming that the same climate forcing occurred during a climatic event at a regional scale, different responses of glaciers are more likely driven by microclimates surrounding individual glaciers caused by geomorphometric characteristics (Furbish and Andrews 1984). Therefore, it is of great importance to investigate the geomorphometric controls on variations in glacial extents.

The Tien Shan, a large mountain range in arid and semiarid regions of central Asia, is well known as the "Water Tower of Central Asia" (Sorg et al. 2012). The large inventory of mountain glaciers in this mountain range provides vital water resources to the local population and ecosystems (Bishop et al. 2011; Gao et al. 2013; Farinotti et al. 2015). Since the end of the Little Ice Age (LIA) around the 1890s, most glaciers in the Tien Shan have been retreating extensively with an accelerated recession rate that has occurred notably in the last few decades (Bolch 2007; Narama et al. 2010; Sorg et al. 2012). Changes in climate conditions are the main causes of the glacier recession. V. B. Aizen et al. (2007) noted that an increase in air temperatures and changes in precipitation partitioning (rain replacing snow at high elevations) have led to negative mass balance of glaciers and changed river runoff regimes in central Asia. Located at the confluence of the midlatitude westerlies and the Siberian high-pressure system, glaciers and rivers in the Tien Shan are sensitive to the temporal variations in the dominance of these systems (Benn and Owen 1998; E. M. Aizen et al. 2001; F. H. Chen et al. 2008). As much effort has been devoted to understanding the linkage between glacier change and climate change, studies have also investigated how glacier changes are affected by geomorphometric factors. For example, studies around the world have shown a consistent pattern that small glaciers have experienced relatively larger proportional changes than large glaciers in the past decades (e.g., S. Y. Liu et al. 2003; Ye et al. 2003; Bhambri et al. 2011; K. Li et al. 2011; Cogley 2014; Y. N. Li and Li 2014; Q. Liu et al. 2015). The fact that more glaciers exist with poleward aspects indicates that equator-ward facing slopes receive more solar radiation to discourage glacier preservation (Evans 2006b). In the Tien Shan, we previously examined the effect of local factors on glacier area and equilibrium-line altitude (ELA) changes within a small region and found that the glacier area and mean elevation are the two main factors in the relative area changes, whereas ELA changes are not strongly associated with local factors (Y. N. Li and Li 2014). Detailed studies on geomorphometric controls in glacier change are still limited in the Tien Shan, although a glacier inventory (e.g., Glacier Inventory of China [GIC]) has been updated and is freely available (Y. F. Shi, Liu, and Kang 2009; S. Y. Liu et al. 2015).

This study focuses on the glacier change since the LIA, a cold era during the last millennium, approximately between AD 1350 and 1890 (Grove 2004). Most studies in the Tien Shan have been conducted for recent decades based on remotely sensed data, but little is known about glacial recession since the LIA. Here, we aim to answer two research questions: (1) How much glacier area has been reduced across three mountain ranges in the eastern Tien Shan from the LIA to present (2006–2010)? and (2) What geomorphometric factors, including glacier area, slope, aspect, shape, elevation, and hypsometry, can be used to explain the variance in glacier area changes?

Study Area

Formed by the collision of the Indian and Eurasian continental plates about 40 to 50 million years ago (Yin and Harrison 2000), the Tien Shan is an ~2,500-km-long mountain series stretching from the western boundary of Kyrgyzstan across the Xinjiang Uyghur Autonomous region in China. The relatively higher, western part of the Tien Shan is recognized as the Kyrgyz Tien Shan, and to the east, approximately two thirds of the total length (~1,700 km) lies within Xinjiang, China. Our study area includes the mountain ranges of the eastern Tien Shan in China, ranging approximately from 85°40′E to 94°50′E and from 42°40′N to 44°00′N (Figure 1). This area includes many individual ranges, most of which reach about 4,000 m above sea level (a.s.l.), and is characterized with a sharp contrast of landscapes of high mountains, intervening valleys, and desert basins (V. B. Aizen et al. 1997; Ye et al. 2005). Glaciers are developed at high elevations and play an important role in the hydrologic

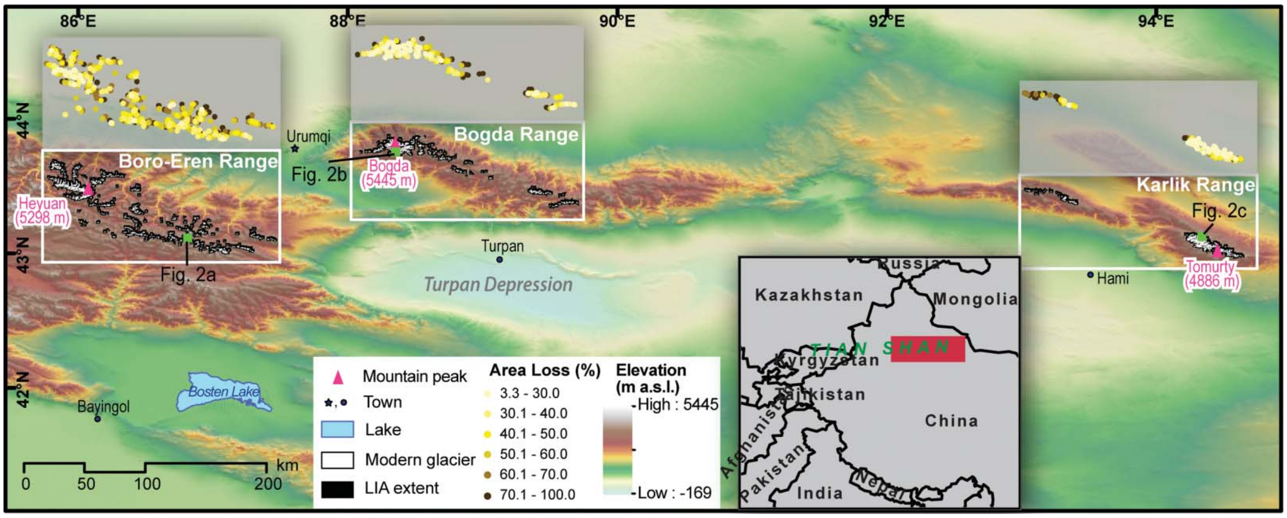

Figure 1. Study area of the eastern Tien Shan (red block on the inset map) and three subregions (white-outlined boxes). The spatial pattern of relative area change is shown using color-graded dots in gray boxes corresponding to each subregion. m a.s.l. = meters above sea level. (Color figure available online.)

cycle, water balance, ecosystems, and socioeconomic development of central Asia. Most glaciers in the study area are clean-ice glaciers, with less than ten glaciers identified as debris-covered glaciers in the GIC (Guo et al. 2014). Glacier types include valley glaciers, hanging glaciers, and cirque glaciers. Three subregions were defined based on the clustering of glacier distribution, separated by two passes of 1,100 m a.s.l. and 860 m a.s.l. in elevation (Figure 1). From west to east, the first subregion is named the Boro-Eren Range (coded BE), which include the eastern Borohoro Mountains and the Eren Habirga Mountains; its highest peak is Heyuan (5,298 m a.s.l.). The second subregion is the Bogda Range (coded BG), located adjacent to the regional capital city Urumqi, and its highest peak is Bogda (5,445 m a.s.l.). The third subregion, the Karlik Range (coded KL), is at the eastern end of the Tien Shan, with relatively fewer glaciers, and the highest peak is Tomurty (4,886 m a.s.l.).

Data and Methods

Data Sets and Data Processing

The outlines of contemporary glaciers were obtained from the Second GIC (Guo et al. 2014), which provides detailed information for each glacier in China. Glacier coverage in the Second GIC was derived from multiple satellite images (Landsat TM/ETM+, ASTER, and SPOT imagery) that were acquired between 2005 and 2010 (S. Y. Liu et al. 2015). The boundaries of contemporary glaciers in our study area (Figure 1) were solely delineated from Landsat TM/ETM+ scenes between 2006 and 2010. The horizontal error of these glacier boundaries is ±30 m (Guo et al. 2014; S. Y. Liu et al. 2015).

The LIA glacial extents were manually delineated in Google Earth (Figure 1; Y. N. Li, Li, Chen, et al. 2016). We defined the outermost fresh and unvegetated moraine in front of glaciers as the maximum extent of LIA glaciers and mapped them in the three mountain ranges of the eastern Tien Shan based on the geomorphic location and relationship, morphology, vegetation cover, and weathering characteristics. Numerical dating of the LIA moraines has been conducted at a few sites in the eastern Tien Shan. For example, the fresh-looking moraine in front of Glacier No. 1 in the BE subregion is well constrained to LIA ages (~430 ± 100 years) using cosmogenic ^{10}Be exposure dating recently (Y. K. Li et al. 2014; Y. N. Li, Li, Harbor, et al. 2016; Figure 2A). Previous studies using other methods, such as lichenometry and radiocarbon dating, also assigned LIA ages to the outermost moraine at this site. J. Chen (1989) dated three moraine ridges at this Glacier No. 1 site to 472 ± 20 years (outermost), 233 ± 20 years, and 139 ± 20 years (innermost) using lichenometry, and Yi et al. (2004) used radiocarbon dating of organic calcium oxalate coatings from the outermost moraine and obtained ages of 460 ± 120 years and 490 ± 120 years (recalculated in Xu and Yi 2014). In the Karlik Range, Y. X. Chen et al. (2015) reported an older moraine

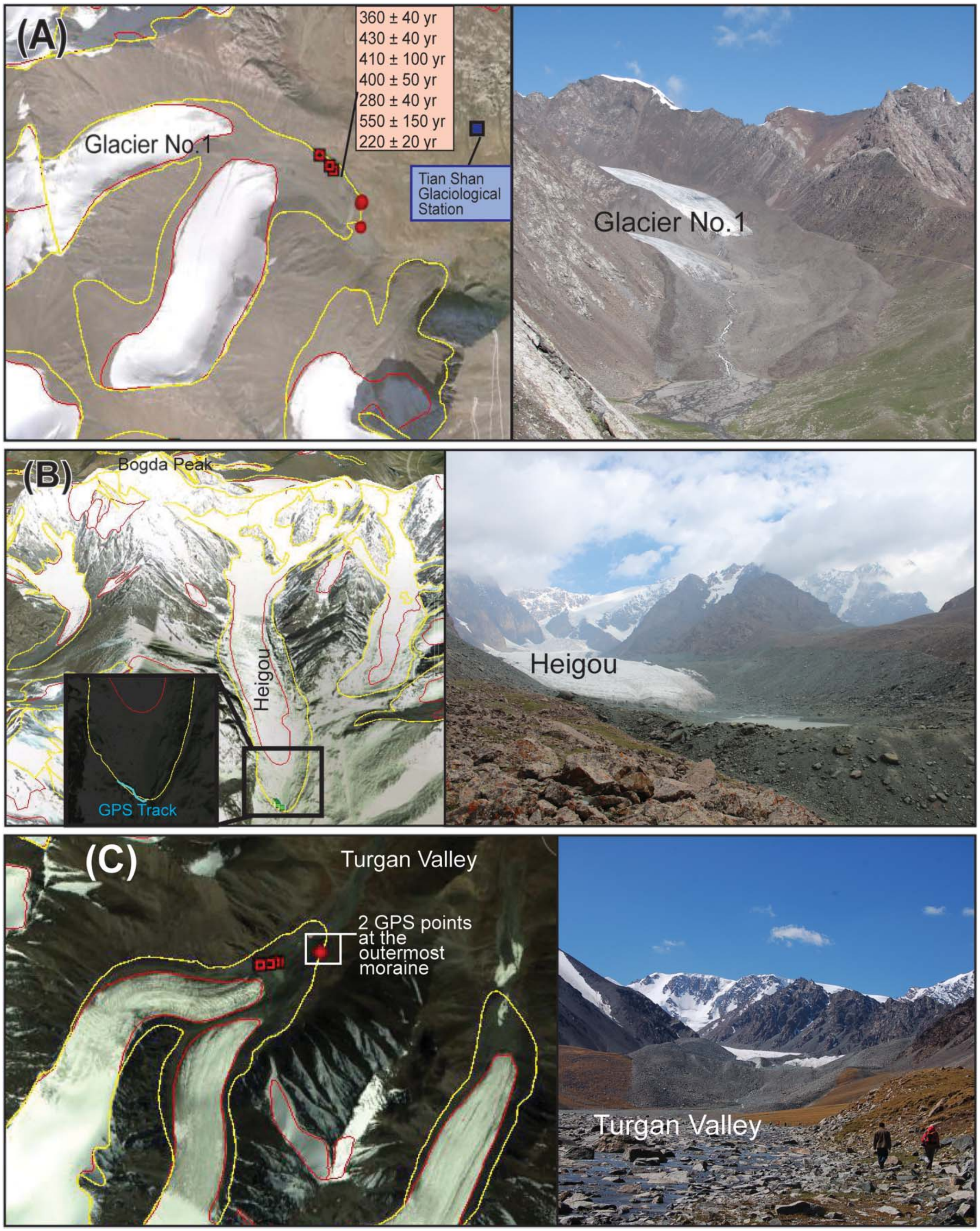

Figure 2. Examples of contemporary glaciers and delineated LIA moraines in Google Earth and in field photos: (A) The Urumqi River headwaters area in the Boro-Eren subregion, with seven cosmogenic ^{10}Be ages indicating the LIA moraine age (Y. K. Li et al. 2014; Y. N. Li, Li, Harbor, et al. 2016). (B) The Heigou Valley in the Bogda subregion, with a GPS receiver track route to validate the delineation of LIA moraine. (C) The Turgan Valley in the Karlik subregion, with two GPS points collected at the outermost fresh moraine (modified from Figures 3 and 4 in Y. N. Li, Li, Chen, et al. 2016). LIA = Little Ice Age; GPS = Global Positioning System. (Color figure available online.)

age of 790 ± 300 years (recalculated in Y. N. Li, Li, Harbor, et al. 2016) based on eleven ^{10}Be exposure ages from the fresh moraines at the Turgan Valley. The manually delineated LIA moraines were saved as Keyhole Markup Language files in Google Earth and converted into shapefiles for further processes in

ArcGIS. The detailed delineation procedure can be found in Y. N. Li, Li, Chen, et al. (2016). To assess the accuracy of our delineated LIA extent of glaciers, we applied a revised automated proximity and conformity analysis (R-APCA; Y. K. Li, Napieralski, and Harbor 2008) to quantify the offset between our field Global Positioning System (GPS) measurements and delineations from Google Earth (Figure 2). The average offsets were 10.5 m, 9.4 m, and 9.1 m at sampled sites in the three subregions, respectively. Hence, the horizontal error of our delineated LIA glacial extents is about ±10 m. This error estimate does not include the potential identification error that occurred in the boundary extraction processes.

We used the Shuttle Radar Topography Mission (SRTM) digital elevation model (DEM; 30 m) downloaded from USGS EarthExplorer (earthexplorer.usgs.gov) to calculate the geomorphometric factors for each glacier. We applied a cubic convolution algorithm to fill some void cells with no data in the original 30-m SRTM DEM. Glacier area was derived directly for both the contemporary and LIA glacier layers in ArcGIS. The area change was then calculated as the difference between glacier areas at these two times. In case of an LIA glacier that had split into individual contemporary glaciers, the change was based on the difference between the total area of individual contemporary glaciers and their corresponding LIA glacier. The change in glacier area might not reflect the ice volume loss but is still a good indicator of glacier change, especially when no ice thickness data are available. To accommodate varied sizes of glaciers, we calculated the relative change of glacier area (in percentage) using the following equation:

$$\Delta A = \left(1 - \frac{\sum A_M}{A_{LIA}}\right) * 100, \tag{1}$$

where ΔA is the relative area change (%); A_M is the area of contemporary glacier(s), and A_{LIA} is the glacier area during the LIA.

We used the method described in Bolch, Menounos, and Wheate (2010), Wei et al. (2014), and S. Y. Liu et al. (2015) for error analysis of glacier area changes. The error of glacier area ε_i is defined as

$$\varepsilon_i = \frac{N * \lambda_i^2}{2}, \tag{2}$$

where N is the number of cells intersecting with the glacier's outline, λ_i is the line pixel error, and i refers to the contemporary or LIA time period. The error in absolute area change $\varepsilon_{(A_{LIA} - A_M)}$ from LIA to present is defined as

$$\varepsilon_{(A_{LIA} - A_M)} = \sqrt{\varepsilon_M^2 + \varepsilon_{LIA}^2} \tag{3}$$

and the error in relative area change $\varepsilon_{\Delta A}$ is defined as

$$\varepsilon_{\Delta A} = \left(1 - \frac{A_M}{A_{LIA}}\right) * \sqrt{\left(\frac{\varepsilon_{LIA}}{A_{LIA}}\right)^2 + \left(\frac{\varepsilon_M}{A_M}\right)^2} * 100. \tag{4}$$

Geomorphometric Factors and Statistical Analysis

In addition to glacier area, we derived aspect, slope, shape, median elevation, and hypsometry, based on the LIA glacier polygons and the DEM in ArcGIS. To incorporate the spatial difference in glacier area loss, the longitude of the centroid ("Easting") of each glacier was added as another factor (Table 1). To examine the statistical relationships between these seven factors and relative glacier area change, we used partial least squares regression (PLSR) because this model accounts for multicollinearity between independent variables and has shown stronger explanatory capacity, compared to principal components analysis and multiple regression (Kemsley 1996; Carrascal, Galván, and Gordo 2009; Yan et al. 2013; Z. Shi et al. 2014). PLSR uses the most important linear combinations (components) in the regression equation, which is achieved by maximizing the covariance between the dependent variable and all possible linear functions of independent variables (Abdi 2003). In our model, the relative glacier area change (ΔA) is the dependent variable (Y), and seven factors are independent variables (X). Glacier area data are highly skewed toward small values (Figure 3A), so they were logarithmic transformed for normal distribution and ln(Area) was used in the regression. Given the circular and continuous nature of the aspect factor, we adopted the method described in Evans (2006a, 2006b, 2011) to transform it into cosine and sine using the first harmonic of a Fourier regression.

Several parameters were used to measure the explanatory and predictive ability of the PLSR model (Abdi 2003; Wold et al. 2004). R^2 is the coefficient of determination and represents the amount explained. Q^2 is the cross-validated R^2 and represents the amount "predicted," defined as (1 – *PRESS*/*SS*), where *PRESS* is predictive residual sum of squares and *SS* is the sum

Table 1. Information of geomorphometric variables derived for the LIA glacial extents

Factor	Variable name	Unit	Summary statistics	Calculation source and method	Note
Glacier area	Area	m^2	—	Calculated using glacier polygons, logarithmic transformed for normal distribution.	It reflects glacier size.
Median elevation	Elevation	M	Median	Derived based on DEM	It reflects glacier's altitudinal location.
Surface slope	Slope	°	Mean	Derived based on DEM	Slope can range from 0° to 90°.
Surface facing	Aspect	°	Directional mean	Derived based on DEM	Aspect spans clockwise from 0° (due north) to 360° (again due north). We calculated the cosine and sine of aspect using Fourier regression.
Distance east	Easting	°	—	Longitude of the centroid of glaciers	It records the longitudinal locations of glaciers in our study area.
Hypsometric integral	HI	N/A	Mean	$\frac{Elev_{mean} - Elev_{min}}{Elev_{max} - Elev_{min}}$	Hypsometry is a simplified factor representing mass balance distribution, ranging from 0 to 1. Small values indicate more area or mass distributed at low elevations and vice versa.
Shape index	Shape	N/A	—	$\frac{D_{min}}{D_{max}}$	Shape is the ratio of largest diameter to the smallest diameter orthogonal to it. It ranges from 0 (extremely elongated) to 1 (equiaxed).

Note: LIA = Little Ice Age; DEM = digital elevation model.

of squares of Y corrected for the mean (Wold et al. 2004). R^2_{cum} is the cumulative R^2 over the selected X variables, and Q^2_{cum} is the cumulative Q^2 over all of the selected PLSR components. The root mean squared error of prediction (RMSEP) is another parameter that contains useful information to calibrate and develop the regression model and is calculated as

$$\text{RMSEP} = \sqrt{\frac{\sum_{i=1}^{n}\left(\bar{y}_{\text{predicted}} - y_{\text{observed}}\right)^2}{n}}. \tag{5}$$

In a PLSR model, the relative importance of each variable is given by the variable importance for the projection (VIP). Variables with larger VIP values are the most relevant for explaining the dependent variable. The regression coefficients reveal the direction and strength of the impact of each variable in the PLSR model. PLSR was performed for glaciers in the entire study area, as well as in each of the three subregions, to examine whether different dominating factors exist in explaining local glacier change. All statistical analyses were performed using R (Ihaka and Gentleman 1996; Björn-Helge and Wehrens 2007).

Results and Discussion

Geomorphometry and Glacier Changes Since the LIA

The total number of delineated LIA glacial extents is 640, corresponding to 865 contemporary glaciers in the Second GIC in the eastern Tien Shan (Table 2). The summary statistics and frequency distribution of geomorphometric features of the 640 LIA glaciers are illustrated in Figure 3. Glacier area has a left-skewed distribution due to the domination of glaciers <2.0 km^2 (550 out of 640, 86 percent), although the range of glacier area is from 0.1 km^2 to 17.4 km^2 (both minimum and maximum values are from the BE subregion; Figure 3A). The mean slope values of these 640 LIA glaciers are likely normally distributed with a mean of 26.6° and a standard deviation of 4.6° (Figure 3B). The median elevations show a slightly left-skewed but close to normal distribution, with a mean of 3,826 m a.s.l. and a standard deviation of 172 m (Figure 3C). The lowest median glacier elevation (3,369 m a.s.l.) is more than 1,000 m lower than the highest one (4,382 m a.s.l.), and both are in the BE range. The shape index ranges from 0.17 to 0.90, with a mean and median of ~0.54

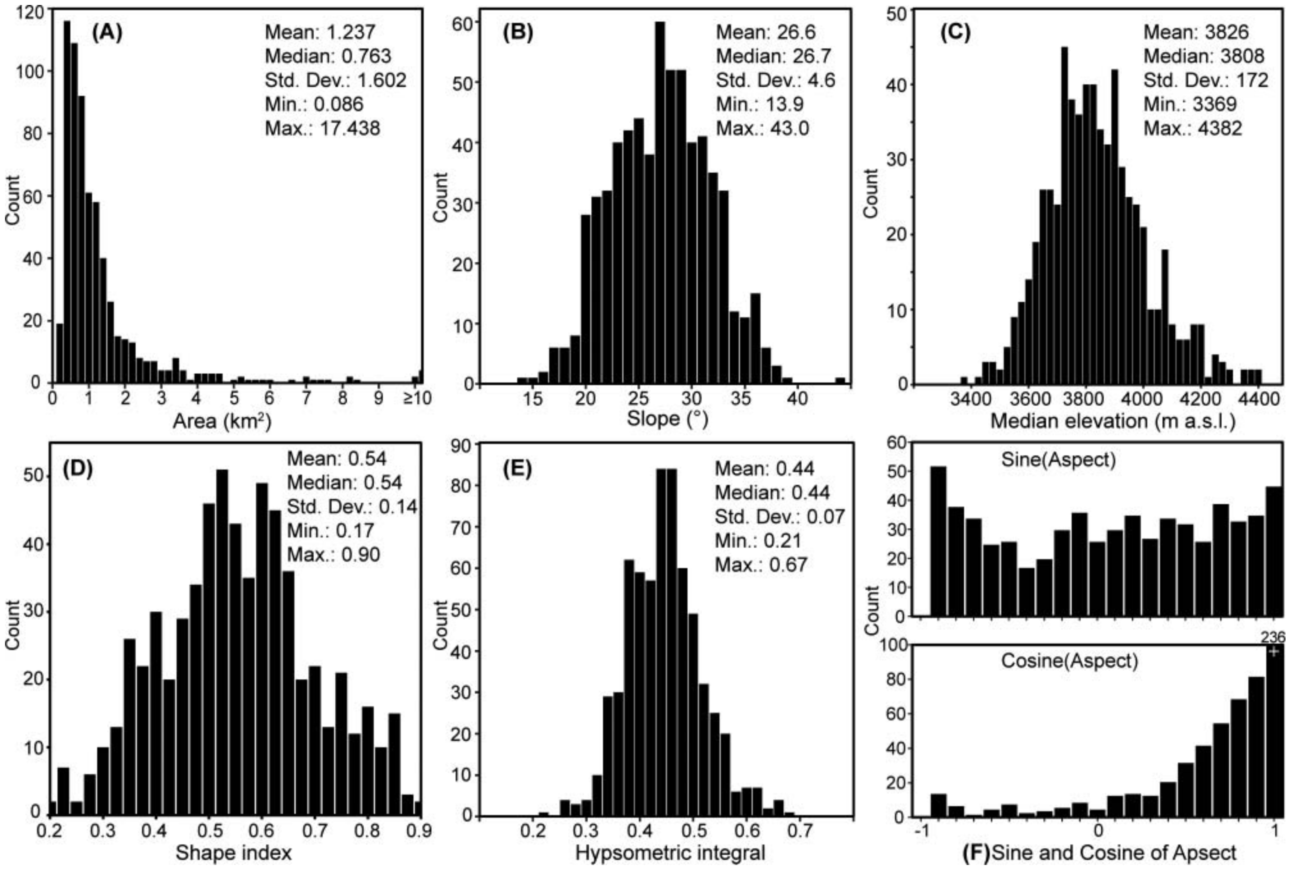

Figure 3. Frequency distribution of six geomorphometric factors: (A) area, (B) slope, (C) median elevation, (D) shape index, (E) hypsometric integral, and (F) sine and cosine of aspect. The sample size is 640.

(Figure 3D). The hypsometric integral (HI) values show a narrow bell-shaped distribution with the same mean and median value of 0.44 (Figure 3E). This might be attributed to the similar geologic background of these alpine glaciers in the study region, but such hypsometry of Tien Shan glaciers could be distinct from that of other glaciated landscapes (Brocklehurst and Whipple 2004). The aspect of glaciers was transformed to Sin(Aspect) and Cos(Aspect), two variables, and the sine term measures east–west differences, whereas the cosine term measures north–south differences (Evans 2006b). As shown in Figure 3F, our glaciers show no apparent east–west contrast, whereas there is a big difference in amount of north-facing and south-facing glaciers. Most glaciers (519 out of 640, 81 percent) are with north-, northeast-, and northwest-facing directions (Figure 4A).

The total area of these glaciers decreased from 791.6 ± 18.7 km^2 during the LIA to 483.9 ± 31.2 km^2 in 2006 to 2010, with a reduction of 38.9 ± 2.7 percent. This reduction percentage represents a minimum estimate of glacier area loss because some LIA glaciers that might have completely disappeared are not included in

Table 2. Comparison of the LIA glacial extents and contemporary glaciers in the eastern Tien Shan

	LIA		Present-day			
	No.	Area (km^2)	No.	Area (km^2)	Absolute area loss (km^2)	Relative area loss (%)
Boro-Eren	392	432.1 ± 10.6	541	244.4 ± 16.9	187.7 ± 20.0	43.4 ± 3.2
Bogda	168	201.1 ± 4.7	202	129.0 ± 8.1	72.1 ± 9.4	35.9 ± 2.4
Karlik	80	158.4 ± 3.3	122	110.6 ± 6.2	47.8 ± 7.0	30.2 ± 1.8
Total	640	791.6 ± 18.7	865	483.9 ± 31.2	307.7 ± 36.4	38.9 ± 2.7

Note: LIA = Little Ice Age.

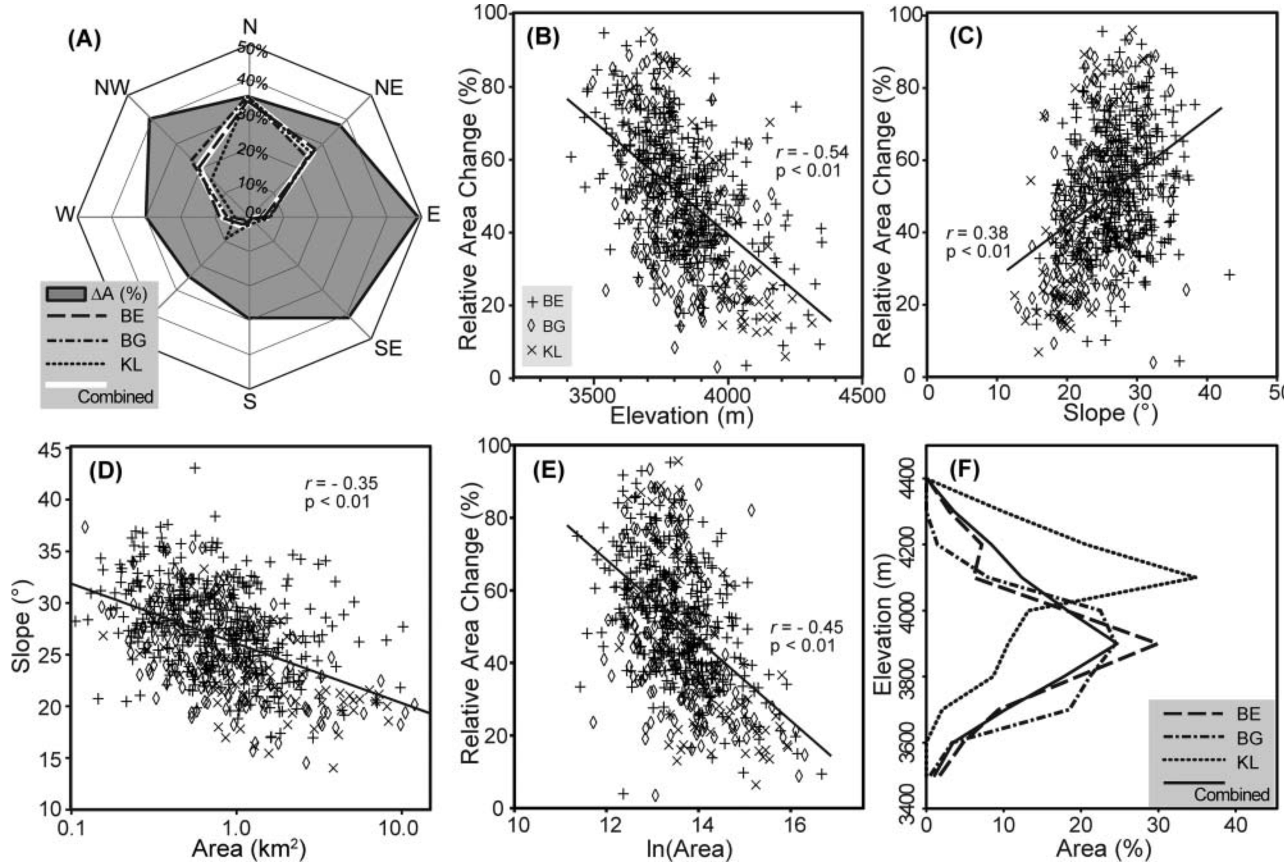

Figure 4. Diagrams and scatter plots to show some important relationships between the relative area change and geomorphometric variables: (A) ΔA vs. aspect; (B) ΔA vs. elevation; (C) ΔA vs. slope; (D) slope vs. area; (E) ΔA vs. ln(area); and (F) area distribution along elevation bins. In (A), both percentages of glaciers at eight directions and the relative area change share the same scale from 0 to 50 percent. *Note*: BE = Boro-Eren Range; BG = Bogda Range; KL = Karlik Range.

the calculation. For the three subregions, BE contains 541 contemporary glaciers that correspond to 392 LIA glaciers, more than half of the total numbers. BE contemporary glaciers have an area of 244.4 ± 16.9 km^2, accounting for about half of the total area. BG is a smaller range compared to BE, and it has 202 glaciers with an area of 129.0 ± 8.1 km^2, corresponding to 168 LIA glaciers. KL is the smallest region with 122 contemporary glaciers (corresponding to 80 LIA glaciers) and a total area (110.6 ± 6.2 km^2) similar to the BG glacier area (Table 2). A west–east decreasing trend is observed in relative area loss in three subregions, ranging from 43.4 ± 3.2 percent, 35.9 ± 2.4 percent, to 30.2 ± 1.8 percent in BE, BG, and KL, respectively.

Important Geomorphometric Factors

Different settings of area, slope, aspect, elevation, shape, and hypsometry of a glacier could influence its response sensitivity to climate change. Pearson's correlation analysis shows pairwise correlations among these independent variables and relative area change (Table 3). For 640 LIA glaciers, the relative area change (ΔA) is correlated with six variables (area, elevation, slope, cosine A, easting, and HI) at the 0.05 significance level. A positive correlation is observed between relative area change and slope, and negative correlations exist between relative area change and area, elevation, cosine A, easting, and HI.

To deduce the relative importance of these geomorphometric variables on glacier changes, we performed the PLSR model on 640 glaciers over the study region (Table 4). Results show that the minimum RMSEP and maximum Q^2 were obtained with the first four components, and the addition of any more components produced an insignificant increase in amount explained because the other components were not strongly correlated with the residuals of the dependent variable. The first component explained 29.22 percent of the total variance, and the addition of the other three components led to a cumulative explained variance of 49.47 percent and a maximum Q^2 of 0.481 (Table 4).

Table 3. Correlation matrix of the relative area change and eight independent variables

	△A	Area	Elevation	Slope	Cosine A	Sine A	Easting	HI	Shape
△A	1								
Area	−0.45**	1							
Elevation	−0.54**	0.22**	1						
Slope	0.38**	−0.35**	−0.07	1					
Cosine A	−0.09*	0.11**	0.04	−0.05	1				
Sine A	0.05	−0.02	−0.02	−0.02	−0.03	1			
Easting	−0.19**	0.15**	0.23**	−0.38**	0.01	−0.04	1		
HI	−0.20**	−0.02	0.44**	0.21**	−0.03	−0.02	0.07	1	
Shape	0.05	0.02	0.07	0.16**	0.04	−0.02	0.04	0.10**	1

Note: HI = hypsometric integral.
*Indicates significance at the 0.05 level ($p < 0.05$)
**Indicates significance at the 0.01 level ($p < 0.01$).

Table 5 shows the composition of only the components that entered the model when minimum RMSEP and maximum Q^2 were reached, in the form of linear combinations of selected predictor variables (geomorphometric factors). In the model of 640 glaciers from the entire study area, the first component is elevation, with a PLSR weight of –1.0; the second component is dominated by slope, with a positive weight; the third component is mainly on easting with a positive weight; and the fourth component is mostly loaded with area and easting, both with negative weights (Table 5). The weight values are indicators for how contributive individual variables are in each component in prediction of relative area change. The variable with the highest VIP value is median elevation (VIP = 2.174), followed by slope (VIP = 1.370). Although some research suggested an arbitrary value of 1 as the threshold to select important variables (Yan et al. 2013; Z. Shi et al. 2014), we feel that it is necessary to include area (VIP = 0.811) and easting (VIP = 0.835) in our regression model for their comparative importance to the rest factors. As the final step in the PLSR model, we only used the four most important variables to generate the regression for the

Table 4. Summary of the partial least squares regression model of relative area change

Response variable	Region	R^2	Q^2	Component	% of explained variance	Cumulative % of explained variance	RMSEP	Q^2_{cum}
Relative area change (△A)	Combined ($n = 640$)	0.49	0.48	1	29.22	29.22	15.87	0.288
				2	12.02	41.24	14.51	0.405
				3	3.10	44.34	14.14	0.435
				4	**5.13**	**49.47**	**13.54**	**0.481**
				5	0.05	49.52	13.55	0.480
	BE ($n = 392$)	0.49	0.47	1	29.17	29.17	13.99	0.280
				2	7.10	36.27	13.31	0.347
				3	**12.57**	**48.84**	**12.02**	**0.467**
				4	0.21	49.05	12.05	0.465
	BG ($n = 168$)	0.43	0.37	1	19.12	19.12	18.00	0.171
				2	18.64	37.76	16.02	0.342
				3	**5.55**	**43.31**	**15.64**	**0.372**
				4	4.09	43.65	15.69	0.367
	KL ($n = 80$)	0.77	0.74	1	58.09	58.09	15.48	0.560
				2	14.59	72.68	12.60	0.708
				3	**4.24**	**76.92**	**11.99**	**0.735**
				4	0.42	77.30	12.28	0.721

Note: RMSEP = root mean squared error of prediction; BE = Boro-Eren Range; BG = Bogda Range; KL = Karlik Range. Values in bold indicate the number of components to reach minimum RMSEP and maximum Q^2.

Table 5. Variable importance for the projection values and partial least squares regression weights for the relative area change model in the whole study area

Region		Area	Elevation	Slope	Cosine A	Sine A	Easting	HI	Shape
Combined	Coefficient	−6.918	−0.056	0.900	−1.070	1.397	0.496	−0.128	0.175
	VIP	0.811	2.174	1.370	0.208[a]		0.835	0.018	0.021
	W[1]		**−1.000**						
	W[2]			**0.987**			−0.217		
	W[3]	−0.188					**1.310**		
	W[4]	**−0.606**		−0.218	−0.120	0.145	**−0.742**		
BG	Coefficient	−5.101	−0.070	1.376	−4.345	0.263	−0.811	−0.221	0.390
	VIP	0.797	1.872	1.825	0.684[a]		0.189	0.076	0.155
	W[1]		**−1.000**						
	W[2]	−0.102		**0.998**					
	W[3]	**−0.739**		−0.173	−0.654	0.136			
KL	Coefficient	−6.413	−0.073	1.787	−0.613	2.496	−1.222	−0.135	0.213
	VIP	0.643	2.452	1.207	0.260[a]		0.214	0.049	0.066
	W[1]		**−1.000**						
	W[2]	−0.117		**0.999**					
	W[3]	**−0.898**		−0.217	−0.109	0.394			
BE	Coefficient	−7.756	−0.052	0.374	0.216	1.371	0.693	−0.139	0.067
	VIP	1.370	2.181	1.119	0.275[a]		0.188	0.041	0.039
	W[1]		**−1.000**						
	W[2]			**1.028**					
	W[3]	**−0.926**		−0.324		0.145	0.151		

Note: HI = hypsometric integral; BG = Bogda Range; KL = Karlik Range; BE = Boro-Eren Range. The values shown in bold indicate that the PLSR components are mainly loaded on these corresponding variables. [1], [2], [3], and [4] indicate partial least squares regression components 1, 2, 3, and 4, respectively.
[a]The variable importance for the projection of the aspect is combined from the variable importance for the projection of CosA and SinA as $\sqrt{VIP^2_{CosA} + VIP^2_{SinA}}$.

640 LIA glaciers in the study area:

$$\Delta A = 297.383 - 7.024 * \ln(\text{Area}) - 0.057 * \text{Elev.} + 0.883 * \text{Slope} + 0.477 * \text{Easting} \quad (6)$$

The Q^2 and the R^2 of the model are 0.483 and 0.491, respectively.

The positive coefficient of easting is contrary to our observed pattern of declining loss from west to east (Table 2). This is likely due to the highly clustered (thus nonnormal) distribution of glaciers in the study area. After excluding the easting variable in the model, the final regression is

$$\Delta A = 336.202 - 7.046 * \ln(\text{Area}) - 0.055 * \text{Elev.} + 0.788 * \text{Slope} \quad (7)$$

The Q^2 and the R^2 of the model are 0.479 and 0.487, respectively. Compared to Equation 6, the Q^2 and the R^2 only suffered a minuscule decrease, but the variables with the strongest explanatory and predictive abilities are kept. Further removal of variables would significantly reduce the explanatory amount and thus no stepwise regression was conducted after this.

Elevation indirectly affects the mass balance of glaciers as the change in elevation is proportional to the change in temperature (Glickman 2000). The negative correlation and negative regression coefficient indicate that glaciers located at higher elevations tend to have less glacier shrinkage compared with those at lower elevations (Figure 4B). Such a finding is in accordance with the general situation that low temperatures at high elevations help retain ice, whereas relatively higher temperatures at low elevations increase ablation. Our previous test in the Boro-Eren range also found that elevation is one of the key factors to glacier changes (Y. N. Li and Li 2014). The role of elevation in determining glacial melt pattern is also emphasized when modeling future change patterns. Hall and Fagre (2003) simulated future melting as influenced by topography for glaciers in Glacier National Park, Montana, and concluded that among three derived factors, "elevation, which corresponds to temperature, was at least twice as powerful a predictor as either aspect or slope in explaining which cells had melted" (137). Our VIP values show a consistency with their finding.

Slope, as the second important factor in our regression, exhibits a positive relationship with the relative area change (Figure 4C), indicating that glaciers on steeper slopes tend to suffer larger fractions of area loss in the eastern Tien Shan. This is contradictory to the well-recognized relationship between slope and the sensitivity of a glacier to climate change. The general situation is that the same upward shift of the ELA will substantially increase the ablation area when the slope is gentle. Some previous studies have discussed this situation with examples of the Nigardsbreen Glacier in Norway (Oerlemans 1992), the Franz Josef and Fox glaciers in New Zealand (Chinn 1996), and 286 Himalayan glaciers (Scherler, Bookhagen, and Strecker 2011). Some studies also found no correlations between magnitude of glacier shrinkage and slope, such as for 321 glaciers in the North Cascades National Park Complex, Washington (Granshaw and Fountain 2006), and for 489 glaciers in the Svartisen region, northern Norway (Paul and Andreassen 2009). The slope effect on glacier dynamics could show substantial variations due to different evolving glacial landscapes of arbitrary regions. In the eastern Tien Shan, the mean slope exhibits a statistically significant dependence on glacier area ($r = -0.35$, $p < 0.01$) as the greater the slope, the smaller the glacier (Figure 4D). Many small glaciers, located at mountain ridges or cirque headwalls, as remnant patches of former valley glaciers, experience more and accelerated glacier change because the entire glacier might exist below the snow line. For example, Dong et al. (2012) reported that in 2008, the ELA of the Urumqi Glacier No. 1 reached an altitude of 4,168 m a.s.l., close to the glacier summit, implying that almost the whole glacier was ablating.

Many studies have shown that small glaciers tend to lose area relatively faster than large glaciers (e.g., Ye et al. 2003; Paul et al. 2004; Bhambri et al. 2011; K. Li et al. 2011). In the high mountains of central Asia, Bolch (2007) found a strong dependence of the glacier retreat (relative area change from 1955 to 1999) on glacier size in the northern Kyrgyz Tien Shan; Bhambri et al. (2011) reported that smaller glaciers (<1 km^2) lost proportionately about six times more of their ice than larger glaciers (>50 km^2) in the central Himalaya from 1968 to 2006. Although glacier sizes are overall much smaller in the eastern Tien Shan compared to these regions, a similar trend is clearly shown here (Figure 4E), as well as in previous studies of Boro-Eren glaciers (Y. N. Li and Li 2014), Bogda glaciers (K. Li et al. 2011), and Karlik glaciers (Wang, Li, and Gao 2011). It is suggested that small glaciers are more sensitive to changes in climate conditions, whereas large compound glaciers tend to respond more slowly (Bahr et al. 1998; Bolch 2007).

Other geomorphometric factors, including aspect, hypsometry, and shape, are not statistically significant factors to relative area changes in our models but could still play a role in the mechanism of glacier dynamics. Although aspect might affect glaciers by creating variations in solar radiation incidence, temperature, wind, and cloudiness (Evans 2006b), our results show that east- and northwest-facing glaciers have higher area loss than others, whereas north-facing glaciers lost less (Figure 4A). Shape could relate to the confinement and potential mass inputs from avalanching from surrounding slopes (DeBeer and Sharp 2007). It could enhance the sensitivity of a glacier but might not be a direct factor. Hypsometry is a simplified factor representing mass balance distribution (Furbish and Andrews 1984). Our narrowly distributed HI values indicate similar mass balance distribution of most glaciers, which have all ranges of relative area change.

Differences among Three Subregions

For all PLSR models of three subregions, the minimum RMSEP and maximum Q^2 were obtained with the first three components (Table 4). The model for the subregion KL produced an R^2 of 0.77 and Q^2 of 0.74, much higher than these in the other two subregion models (BE: $R^2 = 0.49$, $Q^2 = 0.47$; BG: $R^2 = 0.43$, $Q^2 = 0.37$; see Table 4). The selected geomorphometric factors explained the most variance in relative area change in KL, whereas in BE and BG, less than 50 percent of the variance can be explained. One reason for such subregional differences is the smaller number of glaciers in KL ($n = 80$), whereas the ability of factors to explain variances was dampened by relatively large numbers of glaciers in BE ($n = 392$) and BG ($n = 168$). The importance order of the geomorphometric factors was assessed by VIP values in three subregions, as shown in Table 5. Similar to the entire study area, median elevation is the first in all subregions, and the slope and area are the following important factors. In the BE subregion, median elevation and area are the two factors ranked highest, which is consistent with the findings in our previous test (Y. N. Li and Li 2014). Slope is the second highest ranking factor in both BG and KL, but in BG it is almost equally as important as the median elevation, whereas in KL it is only half of the VIP value of the median elevation. Based on the hypsometries as depicted in Figure 4F, KL glaciers show a distinctive curve from other subregions and the entire area, indicating more glaciers distributed at higher altitudes.

The variation in responses of glaciers implies influences from geomorphometric factors as well as other features that could cause local climate differences. The unexplained portions in the models are possibly subject to differences in shade, wind redistribution, avalanching, and other processes, which could modify incoming solar radiation and snow accumulation of a glacier. Unfortunately, these contributors to glacier changes are difficult to quantify, especially for large amounts of glaciers, and were not analyzed in this study.

Other than different roles of important geomorphometric factors within subregions, the easting factor did not show significance in statistical models. Small VIP values (<0.215; Table 5) in the BE, BG, and KL subregions indicate a limited effect of longitudinal location at a local level. The overall decline of relative glacier area changes from west to east was observed (Table 2), which might suggest a spatial pattern of climatic controls across the eastern Tien Shan. In general, the westerlies transport moisture from large water bodies such as the Caspian Sea and Aral Sea in the west, and the orographic effect of the Tien Shan reduces the moisture amount and forms a west–east gradient of precipitation across these mountain ranges (Sorg et al. 2012). Several studies have noted that during past glacial stages, the extent of glaciers in the central Asian mountains is influenced by shifting dominance of the westerlies (Kreutz et al. 1997; Benn and Owen 1998; Gong and Ho 2002; V. B. Aizen et al. 2006). For example, significant glacier advances during Marine Oxygen Isotope Stages (MIS) 4 and MIS 3 in central Asia were accounted for by abundant precipitation carried by the westerlies (Zech 2012; Y. K. Li et al. 2014), whereas arid conditions during the global last glacial maximum (~MIS 2) in the Tien Shan helped to explain the relatively restricted glacial advances (Abramowski et al. 2006; Narama et al. 2007; Koppes et al. 2008). As the westerlies become less powerful eastwards, the Siberian High dominates and delivers cold air masses to the eastern end of Tien Shan. A generally stronger Siberian High since the LIA (Gong and Ho 2002; D'Arrigo et al. 2005) counteracted the effect of limited precipitation; hence, it is suggested that in the Karlik Range, the lower temperature and relatively higher altitudes resulted in less glacier retreats than in other parts of study region (Y. X. Chen et al. 2015; Y. N. Li, Li, Harbor, et al. 2016). Knowledge of climate conditions in three subregions during the LIA is still limited, so it prevents us from investigating how glaciers behaved differently in relation to the in situ climate conditions. To better quantify climate controls on glacier changes across the Tien Shan, we need further work and more information on past climate and robust numerical models at a detailed subregional spatial scale.

Conclusions

This study investigated the glacier changes since the LIA in the eastern Tien Shan based on the Second GIC data, delineations of LIA extents from Google Earth, and a 30-m SRTM DEM. The total area of glaciers decreased from 791.6 $\pm$ 18.7 km^2 during the LIA to 483.9 $\pm$ 31.2 km^2 during 2006 to 2010, a loss of 38.9 $\pm$ 2.7 percent. Within the whole study area and each subregion, large variability in relative glacier area change suggests that local geomorphometric settings are important in controlling the behavior of glaciers. To quantify the importance of such local factors, glacier area, aspect, slope, shape, median elevation, hypsometry, as well as the longitude were extracted for each LIA glacier and used as predictor variables, whereas the relative area change of each glacier from LIA to present was used as the response variable. Although Pearson's correlation test showed the significance of each factor in relation to relative area change, the PLSR model revealed that the variance in the response variable was attributed mainly to three factors: glacier elevation, slope, and area. Models for three subregions showed similar results to the whole area. The predictive ability is relatively higher in the Karlik, the easternmost subregion. Overall, from the western to the eastern subregions, the area loss exhibits a decreasing trend. The influence of climatic changes on glacier changes might vary spatially: The western part is more influenced by the westerlies, whereas the eastern regions are more under the impact of the Siberian High in the past few hundreds of years. To better understand the linkage among glacier, geomorphometry, and climate, we need more data and further modeling work in the eastern Tien Shan.

References

Abdi, H. 2003. *Partial least square regression (PLS regression)*. Thousand Oaks, CA: Sage.

Abramowski, U., A. Bergau, D. Seebach, R. Zech, B. Glaser, P. Sosin, P. W. Kubik, and W. Zech. 2006. Pleistocene glaciations of central Asia: Results from

^{10}Be surface exposure ages of erratic boulders from the Pamir (Tajikistan), and the Alay-Turkestan range (Kyrgyzstan). *Quaternary Science Reviews* 25 (9–10): 1080–96.

Aizen, E. M., V. B. Aizen, J. M. Melack, T. Nakamura, and T. Ohta. 2001. Precipitation and atmospheric circulation patterns at mid-latitudes of Asia. *International Journal of Climatology* 21 (5): 535–56.

Aizen, V. B., E. M. Aizen, J. M. Melack, and J. Dozier. 1997. Climatic and hydrologic changes in the Tien Shan, Central Asia. *Journal of Climate* 10 (6): 1393–1404.

Aizen, V. B., E. M. Aizen, A. B. Surazakov, and V. A. Kuzmichenok. 2006. Assessment of glacial area and volume change in Tien Shan (central Asia) during the last 150 years using geodetic, aerial photo, ASTER and SRTM data. *Annals of Glaciology* 43:202–13.

Aizen, V. B., V. A. Kuzmichenok, A. B. Surazakov, and E. M. Aizen. 2007. Glacier changes in the Tien Shan as determined from topographic and remotely sensed data. *Global and Planetary Change* 56 (3): 328–40.

ArcGIS. Version 10.1. Redlands, CA: Esri.

Bahr, D. B., W. T. Pfeffer, C. Sassolas, and M. F. Meier. 1998. Response time of glaciers as a function of size and mass balance: 1. Theory. *Journal of Geophysical Research: Solid Earth* 103 (B5): 9777–82.

Benn, D., and L. Owen. 1998. The role of the Indian summer monsoon and the mid-latitude westerlies in Himalayan glaciation: Review and speculative discussion. *Journal of the Geological Society* 155 (2): 353–63.

Bhambri, R., T. Bolch, R. K. Chaujar, and S. C. Kulshreshtha. 2011. Glacier changes in the Garhwal Himalaya, India, from 1968 to 2006 based on remote sensing. *Journal of Glaciology* 57 (203): 543–56.

Bishop, M. P., H. Björnsson, W. Haeberli, J. Oerlemans, J. F. Shroder, M. Tranter, V. P. Singh, P. Singh, and U. K. Haritashya. 2011. *Encyclopedia of snow, ice and glaciers*. Berlin: Springer Science & Business Media.

Björn-Helge, M., and R. Wehrens. 2007. The PLS package: Principal component and partial least squares regression in R. *Journal of Statistical Software* 18 (2): 1–24.

Bolch, T. 2007. Climate change and glacier retreat in northern Tien Shan (Kazakhstan/Kyrgyzstan) using remote sensing data. *Global and Planetary Change* 56 (1): 1–12.

Bolch, T., B. Menounos, and R. Wheate. 2010. Landsat-based inventory of glaciers in western Canada, 1985–2005. *Remote Sensing of Environment* 114 (1): 127–37.

Brocklehurst, S. H., and K. X. Whipple. 2004. Hypsometry of glaciated landscapes. *Earth Surface Processes and Landforms* 29:907–26.

Carrascal, L. M., I. Galván, and O. Gordo. 2009. Partial least squares regression as an alternative to current regression methods used in ecology. *Oikos* 118 (5): 681–90.

Chen, F. H., Z. C. Yu, M. L. Yang, E. Ito, S. M. Wang, D. B. Madsen, X. Z. Huang, et al. 2008. Holocene moisture evolution in arid central Asia and its out-of-phase relationship with Asian monsoon history. *Quaternary Science Reviews* 27 (3–4): 351–64.

Chen, J. 1989. Preliminary researches on lichenometric chronology of Holocene glacial fluctuations and on other topics in the headwater of Urumqi River, Tianshan Mountains. *Science in China Series B: Chemistry* 32 (12): 1487–1500.

Chen, Y. X., Y. K. Li, Y. Y. Wang, M. Zhang, Z. J. Cui, C. L. Yi, and G. N. Liu. 2015. Late Quaternary glacial history of the Karlik Range, easternmost Tian Shan, derived from ^{10}Be surface exposure and optically stimulated luminescence datings. *Quaternary Science Reviews* 115:17–27.

Chinn, T. J. 1996. New Zealand glacier responses to climate change of the past century. *New Zealand Journal of Geology and Geophysics* 39 (3): 415–28.

Cogley, J. G. 2014. Glacier shrinkage across High Mountain Asia. *Annals of Glaciology* 57 (71): 41–49.

D'Arrigo, R., G. Jacoby, R. Wilson, and F. Panagiotopoulos. 2005. A reconstructed Siberian High index since A.D. 1599 from Eurasian and North American tree rings. *Geophysical Research Letters* 32 (5): L05705.

DeBeer, C. M., and M. J. Sharp. 2007. Recent changes in glacier area and volume within the southern Canadian Cordillera. *Annals of Glaciology* 46 (1): 215–21.

Delmas, M., Y. Gunnell, and M. Calvet. 2014. Environmental controls on alpine cirque size. *Geomorphology* 206:318–29.

Dong, Z. W., D. H. Qin, J. W. Ren, K. M. Li, and Z. Q. Li. 2012. Variations in the equilibrium line altitude of Urumqi Glacier No. 1, Tianshan Mountains, over the past 50 years. *Chinese Science Bulletin* 57:4776–83.

Evans, I. S. 2006a. Glacier distribution in the Alps: Statistical modelling of altitude and aspect. *Geografiska Annaler: Series A-Physical Geography* 88 (2): 115–33.

———. 2006b. Local aspect asymmetry of mountain glaciation: A global survey of consistency of favoured directions for glacier numbers and altitudes. *Geomorphology* 73 (1–2): 166–84.

———. 2011. Glacier distribution and direction in Svalbard, Axel Heiberg Island and throughout the Arctic: General northward tendencies. *Polish Polar Research* 32 (3): 199–238.

Farinotti, D., L. Longuevergne, G. Moholdt, D. Duethmann, T. Mölg, T. Bolch, S. Vorogushyn, and A. Güntner. 2015. Substantial glacier mass loss in the Tien Shan over the past 50 years. *Nature Geoscience* 8:716–22.

Furbish, D., and J. Andrews. 1984. The use of hypsometry to indicate long-term stability and response of valley glaciers to changes in mass transfer. *Journal of Glaciology* 30 (105): 199–211.

Gao, M., T. Han, B. Ye, and K. Jiao. 2013. Characteristics of melt water discharge in the Glacier No. 1 basin, headwater of Urumqi River. *Journal of Hydrology* 489:180–88.

Glickman, T. S. 2000. *Glossary of meteorology*. Boston: American Meteorological Society.

Gong, D. Y., and C. H. Ho. 2002. The Siberian High and climate change over middle to high latitude Asia. *Theoretical and Applied Climatology* 72 (1–2): 1–9.

Granshaw, F. D., and A. G. Fountain. 2006. Glacier change (1958–1998) in the north Cascades national park complex, Washington, USA. *Journal of Glaciology* 52 (177): 251–56.

Grove, J. M. 2004. *Little ice ages: Ancient and modern*. 2 vols. London and New York: Routledge.

Guo, W., J. Xu, S. Liu, D. Shangguan, L. Wu, X. Yao, J. Zhao, Q. Liu, Z. Jiang, and P. Li. 2014. *The second glacier inventory dataset of China* (Version 1.0). Lanzhou, China: Cold and Arid Regions Science Data Center at Lanzhou.

Hall, M. H., and D. B. Fagre. 2003. Modeled climate-induced glacier change in Glacier National Park, 1850–2100. *BioScience* 53 (2): 131–40.

Ihaka, R., and R. Gentleman. 1996. R: A language for data analysis and graphics. *Journal of Computational and Graphical Statistics* 5 (3): 299–314.

Kemsley, E. 1996. Discriminant analysis of high-dimensional data: A comparison of principal components analysis and partial least squares data reduction methods. *Chemometrics and Intelligent Laboratory Systems* 33 (1): 47–61.

Koppes, M., A. R. Gillespie, R. M. Burke, S. C. Thompson, and J. Stone. 2008. Late Quaternary glaciation in the Kyrgyz Tien Shan. *Quaternary Science Reviews* 27 (7–8): 846–66.

Kreutz, K., P. Mayewski, L. Meeker, M. Twickler, S. Whitlow, and I. Pittalwala. 1997. Bipolar changes in atmospheric circulation during the Little Ice Age. *Science* 277:1294–96.

Li, K., H. Li, L. Wang, and W. Gao. 2011. On the relationship between local topography and small glacier change under climatic warming on Mt. Bogda, eastern Tian Shan, China. *Journal of Earth Science* 22 (4): 515–27.

Li, Y. K., G. N. Liu, Y. X. Chen, Y. N. Li, J. Harbor, A. P. Stroeven, M. Caffee, M. Zhang, C. C. Li, and Z. J. Cui. 2014. Timing and extent of quaternary glaciations in the Tianger Range, eastern Tian Shan, China, investigated using ^{10}Be surface exposure dating. *Quaternary Science Reviews* 98:7–23.

Li, Y. K., J. Napieralski, and J. Harbor. 2008. A revised automated proximity and conformity analysis method to compare predicted and observed spatial boundaries of geologic phenomena. *Computers & Geosciences* 34 (12): 1806–14.

Li, Y. N., and Y. K. Li. 2014. Topographic and geometric controls on glacier changes in the central Tien Shan, China, since the Little Ice Age. *Annals of Glaciology* 55 (66): 177–86.

Li, Y. N., Y. K. Li, Y. X. Chen, and X. Y. Lu. 2016. Presumed Little Ice Age glacial extent in the eastern Tian Shan, China. *Journal of Maps*. Advance online publication. http://dx.doi.org/10.1080/17445647.2016.1158595

Li, Y. N., Y. K. Li, J. Harbor, G. N. Liu, C. L. Yi, and M. Caffee. 2016. Cosmogenic ^{10}Be constraints on Little Ice Age glacial advances in the eastern Tian Shan, China. *Quaternary Science Reviews* 138:105–18.

Liu, Q., S. Y. Liu, W. Q. Guo, Y. Nie, D. H. Shangguan, J. L. Xu, and X. J. Yao. 2015. Glacier changes in the Lancang River Basin, China, between 1968–1975 and 2005–2010. *Arctic, Antarctic, and Alpine Research* 47 (2): 335–44.

Liu, S. Y., W. X. Sun, Y. P. Shen, and G. Li. 2003. Glacier changes since the Little Ice Age maximum in the western Qilian Shan, northwest China, and consequences of glacier runoff for water supply. *Journal of Glaciology* 49 (164): 117–24.

Liu, S. Y., X. J. Yao, W. Q. Guo, J. L. Xu, D. H. Shangguan, J. F. Wei, W. J. Bao, and L. Z. Wu. 2015. The contemporary glaciers in China based on the Second Chinese Glacier Inventory. *Acta Geographica Sinica* 70 (1): 3–16.

Narama, C., A. Kääb, M. Duishonakunov, and K. Abdrakhmatov. 2010. Spatial variability of recent glacier area changes in the Tien Shan Mountains, Central Asia, using Corona (~1970), Landsat (~2000), and ALOS (~2007) satellite data. *Global and Planetary Change* 71 (1): 42–54.

Narama, C., R. Kondo, S. Tsukamoto, T. Kajiura, C. Ormukov, and K. Abdrakhmatov. 2007. OSL dating of glacial deposits during the last glacial in the Terskey-Alatoo Range, Kyrgyz Republic. *Quaternary Geochronology* 2 (1–4): 249–54.

Oerlemans, J. 1992. Climate sensitivity of glaciers in southern Norway: Application of an energy-balance model to Nigardsbreen, Hellstugbreen and Alfotbreen. *Journal of Glaciology* 38:223–32.

Paul, F., and L. M. Andreassen. 2009. A new glacier inventory for the Svartisen region, Norway, from Landsat ETM+ data: Challenges and change assessment. *Journal of Glaciology* 55 (192): 607–18.

Paul, F., A. Kääb, M. Maisch, T. Kellenberger, and W. Haeberli. 2004. Rapid disintegration of Alpine glaciers observed with satellite data. *Geophysical Research Letters* 31 (21): L21402.

R Development Core Team. *R*. Version 3.2.2. Vienna, Austria: R Development Core Team.

Scherler, D., B. Bookhagen, and M. R. Strecker. 2011. Spatially variable response of Himalayan glaciers to climate change affected by debris cover. *Nature Geoscience* 4 (3): 156–59.

Shi, Y. F., C. H. Liu, and E. Kang. 2009. The Glacier Inventory of China. *Annals of Glaciology* 50 (53): 1–4.

Shi, Z., X. Huang, L. Ai, N. Fang, and G. Wu. 2014. Quantitative analysis of factors controlling sediment yield in mountainous watersheds. *Geomorphology* 226:193–201.

Sorg, A., T. Bolch, M. Stoffel, O. Solomina, and M. Beniston. 2012. Climate change impacts on glaciers and runoff in Tien Shan (Central Asia). *Nature Climate Change* 2 (10): 725–31.

Wang, W., K. Li, and J. Gao. 2011. Monitoring glacial shrinkage using remote sensing and site-observation method on southern slope of Kalik Mountain, eastern Tian Shan, China. *Journal of Earth Science* 22:503–14.

Wei, J., S. Liu, W. Guo, X. Yao, J. Xu, W. Bao, and Z. Jiang. 2014. Surface-area changes of glaciers in the Tibetan Plateau interior area since the 1970s using recent Landsat images and historical maps. *Annals of Glaciology* 55 (66): 213–22.

Wold, S., L. Eriksson, J. Trygg, and N. Kettaneh. 2004. *The PLS method—partial least squares projections to latent structures—and its applications in industrial RDP (research, development, and production)*. Umeå, Sweden: Umeå University.

Xu, X., and C. Yi. 2014. Little Ice Age on the Tibetan Plateau and its bordering mountains: Evidence from moraine chronologies. *Global and Planetary Change* 116:41–53.

Yan, B., N. Fang, P. Zhang, and Z. Shi. 2013. Impacts of land use change on watershed streamflow and sediment yield: An assessment using hydrologic modelling and partial least squares regression. *Journal of Hydrology* 484:26–37.

Ye, B., Y. Ding, F. Liu, and C. Liu. 2003. Responses of various-sized alpine glaciers and runoff to climatic change. *Journal of Glaciology* 49 (164): 1–7.

Ye, B., D. Yang, K. Jiao, T. Han, Z. Jin, H. Yang, and Z. Li. 2005. The Urumqi River source Glacier No. 1, Tianshan, China: Changes over the past 45 years. *Geophysical Research Letters* 32 (21): L21504.

Yi, C., K. Liu, Z. Cui, K. Jiao, T. Yao, and Y. He. 2004. AMS radiocarbon dating of late Quaternary glacial landforms, source of the Urumqi River, Tien Shan—A pilot study of ^{14}C dating on inorganic carbon. *Quaternary International* 121 (1): 99–107.

Yin, A., and T. M. Harrison. 2000. Geologic evolution of the Himalayan–Tibetan orogen. *Annual Review of Earth and Planetary Sciences* 28 (1): 211–80.

Zech, R. 2012. A late Pleistocene glacial chronology from the Kitschi-Kurumdu Valley, Tien Shan (Kyrgyzstan), based on 10Be surface exposure dating. *Quaternary Research* 77 (2): 281–88.

YANAN LI is an Assistant Professor in the Department of Geography at South Dakota State University, Brookings, SD 57007. E-mail: yanan.li@sdstate.edu. Her research interests include glacial geomorphology, paleoclimatology, and terrain analysis.

YINGKUI LI is an Associate Professor in the Department of Geography at the University of Tennessee, Knoxville, TN 37996. E-mail: yli32@utk.edu. His research interests include geomorphology, environmental reconstruction, LiDAR and Earth surface processes, geographic information systems, and spatial analysis.

XIAOYU LU is a PhD student in the Department of Geography at the University of Tennessee, Knoxville, TN 37996. E-mail: xlu14@utk.edu. His research interests include soil erosion, Earth surface processes, remote sensing, and LiDAR.

JON HARBOR is a Professor in the Department of Earth, Atmospheric, and Planetary Sciences at Purdue University, West Lafayette, IN 47907. E-mail: jharbor@purdue.edu. His research interests include geomorphology, water resources, land use and climate change, and geographic education.